

**A THEORETICAL INVESTIGATION OF A POTENTIAL HIGH ENERGY DENSITY COMPOUND
3,6,7,8-TETRANITRO-3,6,7,8-TETRAAZA-TRICYCLO[3.1.1.1^{2,4}]OCTANE**

Guozheng Zhao and Ming Lu*

School of Chemical Engineering, Nanjing University of Science & Technology, Nanjing, Jiangsu, 210094, P. R. China

Recebido em 3/5/12; aceito em 30/10/12; publicado na web em 6/3/13

The B3LYP/6-31G (d) density functional theory (DFT) method was used to study molecular geometry, electronic structure, infrared spectrum (IR) and thermodynamic properties. Heat of formation (HOF) and calculated density were estimated to evaluate detonation properties using Kamlet-Jacobs equations. Thermal stability of 3,6,7,8-tetranitro-3,6,7,8-tetraaza-tricyclo [3.1.1.1^{2,4}]octane (TTTO) was investigated by calculating bond dissociation energy (BDE) at the unrestricted B3LYP/6-31G(d) level. Results showed the N–NO₂ bond is a trigger bond during the thermolysis initiation process. The crystal structure obtained by molecular mechanics (MM) methods belongs to *P2₁/C* space group, with cell parameters *a* = 8.239 Å, *b* = 8.079 Å, *c* = 16.860 Å, *Z* = 4 and ρ = 1.922 g cm⁻³. Both detonation velocity of 9.79 km s⁻¹ and detonation pressure of 44.22 GPa performed similarly to CL-20. According to the quantitative standards of energetics and stability, TTTO essentially satisfies this requirement as a high energy density compound (HEDC).

Keywords: density functional theory; molecular mechanics; TTTO.

INTRODUCTION

In a bid to meet the continuing need for novel high energy density compounds (HEDCs) with high explosive performance and insensitivity, many scientists have devoted considerable effort to designing and synthesizing these over several decades.¹⁻³ For HEDCs, besides high detonation performance, sensitivity is a prerequisite requirement.⁴⁻⁷ HEDCs should be sufficiently safe, stable and reliable to detonate under specific conditions. Thus, good thermal stability and low impact and shock sensitivities are of equal importance to detonation performance, but these requirements are somewhat reciprocally exclusive, with improved insensitivity associated with inferior performance and vice versa. Therefore, the foremost objective is to find the molecule which offers best detonation performance and thermal stability.

Energetic materials of the strained ring and cage families have emerged as a promising new class of explosives in recent years.⁸⁻¹⁰ In this class, octanitrocubane (ONC)¹¹ is a highly energetic explosive, which is the most powerful explosive presently used.¹² The energy performance of ONC calculated at a density of 2.03 g/cm³ yields 20% more energy output than HMX.¹³ The preparation of 1,3,5,7-tetranitroadmantane (TNA) was reported by Sollott.¹⁴ TNA with its high melting point of ca. 350 °C, is likely to be of value as a heat resistant explosive. CL-20 [2,4,6,8,10,12-hexanitrohexaazaisowurtzitane (HNIW)] is another new nitramine explosive, which has 6 N–NO₂ groups in its polycyclic structure, resulting in higher density and heat of formation.¹⁵⁻¹⁷ CL-20 is reported as an attractive highly thermally stable explosive with a decomposition temperature of 228 °C. These strained rings of cage compounds possess a concomitant high heat of formation and density, making them powerful explosives.¹⁸⁻²⁰

The typical characteristic of cage compounds is that they derive most energy from their high heat of formation, in contrast to classical explosives such as TNT and HMX which derive their energy from oxidation of carbon backbone. On the other hand, compounds with compact structure usually have higher densities and can also release additional energy upon detonation as a consequence of the cage strain in these systems. The high heat of formation of cage compounds is combined with the high energy of nitramine explosives.

Reacting with ammonia, glyoxal yields a precursor 3,6,7,8-tetraaza-tricyclo[3.1.1.1^{2,4}]octane, which provides more N–H sites for introducing nitro substituents, and thus generates the new energetic material 3,6,7,8-tetranitro-3,6,7,8-tetraaza-tricyclo[3.1.1.1^{2,4}]octane.

Owing to the difficulties in the synthesis of the molecules under consideration, computer tests become an effective way to design high energy density compounds theoretically.²¹⁻²⁴ The optimization of molecules with high energy and density is the primary step for searching for and synthesizing HEDCs. To date, there is scant information available on TTTO (Figure 1). In the present work, density functional theory and molecular mechanics methods were employed to evaluate the crystal structure and properties of TTTO, such as heat of formation, infrared spectrum, thermodynamic properties, detonation performance and thermal stability. These results showed that TTTO may represent a very promising high energy density compound.

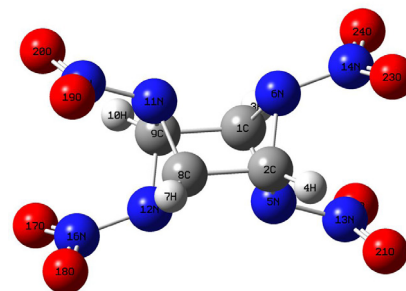


Figure 1. Molecular structure of TTTO

COMPUTATIONAL METHODS

Computations were performed with the Gaussian 03 package at B3LYP/6-31G (d), B3LYP/6-311G(d,p), B3LYP/6-311+G(d,p) and B3P86/6-311+G(d,p) levels.²⁵⁻²⁸ The geometric parameters were optimizable and no constraints were imposed on molecular structure during the optimization process. Vibrational frequencies were calculated for the optimized structures to enable characterization of the nature of stationary points, zero-point energy (ZPE) and thermal

*e-mail: lumingchem@163.com

correction (H_T). The optimized structure was characterized to be a true local energy minima on potential energy surfaces without imaginary frequencies. On the basis of the principle of statistical thermodynamics,²⁹ the standard molar heat capacity ($C_{p,m}^\theta$), standard molar entropy (S_m^θ) and standard molar enthalpy (H_m^θ) from 200 to 800 K were derived from the scaled frequencies using a self-compiled program.

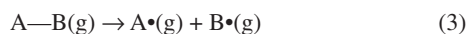
Detonation velocity and pressure are the most important parameters to evaluate detonation characteristics of energetic materials. For explosives with CHNO elements, the Kamlet and Jacobs empirical equations were used to determine these parameters.³⁰

$$P = 1.558NM^{1/2}Q^{1/2}\rho^2 \quad (1)$$

$$D = 1.01(NM^{1/2}Q^{1/2})^{1/2}(1 + 1.30\rho) \quad (2)$$

where P is detonation pressure in GPa, D is detonation velocity in km s^{-1} , N is the number moles of gaseous detonation products per gram of explosive, M is the average molecular weight of the gaseous products, Q is the energy of explosion in J g^{-1} of explosive and ρ is the crystal density in g cm^{-3} . N , M and Q are determined according to the largest exothermic principle,³¹ i.e., for the explosives with CHNO elements, all the N atoms convert into N_2 , the O atom forms H_2O with the H atom first and the remainder forms CO_2 with the C atom. The remainder of the C atom will exist in solid state if the O atom does not satisfy full oxidation of the C atom. The remainder of the O atom will exist in O_2 if the O atom is superfluous.

The strength of bonding, which can be evaluated by the bond dissociation energy, is fundamental to understanding chemical processes.³² BDE is the required energy in homolysis of a bond and is commonly denoted by difference between total energies of product and reactant after zero-point energy correction. The expressions for the homolysis of A—B bond (3) and for calculating its BDE (4) are shown as follows:³³



$$\text{BDE(A—B)}_{\text{ZPE}} = E(\text{A}\cdot)_{\text{ZPE}} + E(\text{B}\cdot)_{\text{ZPE}} - E(\text{A—B})_{\text{ZPE}} \quad (4)$$

where A—B stands for neutral molecules and $\text{A}\cdot$ and $\text{B}\cdot$ for the corresponding product radicals after bond dissociation; BDE(A—B) is the BDE of bond A—B; $E(\text{A—B})_{\text{ZPE}}$, $E(\text{A}\cdot)_{\text{ZPE}}$ and $E(\text{B}\cdot)_{\text{ZPE}}$ are zero-point energy corrected total energies of parent compound and corresponding radicals, respectively.

Because high energy density compounds are usually in condensed phases, especially solid forms, we predicted the possible polymorphs and crystal structure of TTTO by rigorous molecular packing calculations using the polymorph module of Materials Studio.³⁴ The Compass force field is capable of predicting the condensed phase properties by searching the possible molecular packing among the most probable seven space groups ($P2_1/c$, $P-1$, $P2_12_12_1$, $Pbca$, $C2/c$, $P2_1$ and $Pna2_1$).^{35–38}

RESULTS AND DISCUSSION

Molecular geometry and crystal structure

It is useful to examine the geometric structure of the title compound before discussing the various properties. Because of the steric hindrance effect, the N—NO₂ groups all depart from the attached ring plane. This is due to the repulsion between the neighboring nitro group, which rotate oxygen atoms from the molecular plane. Optimized bond lengths of TTTO at the B3LYP/6-31G(d) are listed in Table 1. The C—N bond of TTTO is found to be longer than the normal C—N single bond reported as 1.49 Å,³⁹ while the difference is not significant. Lengths

of N—NO₂ bonds in TTTO are all 1.424 Å, longer than the usual N—N bond lengths (1.35–1.40 Å) in nitramines⁴⁰ because of the electron withdrawing inductive effect of the nitro group. It is proposed that the C—C bonds in TTTO correspond to C1—C9 and C2—C8 bonds, which are all 1.603 Å. Thus, all the C—C bonds in TTTO are much longer than the normal C—C single bond that is reported as 1.54 Å, which are elongated due to the cage strain in the system.

Table 1. Selected bond lengths of TTTO computed at B3LYP/6-31G (d) level^a

Bond	Bond	Bond	Bond	Bond	Bond
C1-C9	1.603	C1-N6	1.499	N13-O22	1.221
C2-C8	1.603	C2-N5	1.499	N14-O23	1.221
N5-N13	1.424	C2-N6	1.499	N14-O24	1.221
N6-N14	1.424	C8-N12	1.499	N15-O19	1.221
N11-N15	1.424	C9-N11	1.499	N15-O20	1.221
N12-N16	1.424	C9-N12	1.499	N16-O17	1.221
C1-N5	1.499	N13-O21	1.221	N16-O18	1.221

^a Bond lengths in Angstroms.

In this study, the crystal density has been predicted from the crystal packing calculations based on the molecular mechanics method.^{41,42} Compass force field,⁴³ capable of producing the gas-phase and condensed-phase properties reliably for a broad range of systems including nitramines such as CL-20,^{44,45} has been employed to predict the crystal structure of TTTO. The approach is based on the generation of possible packing arrangements in all reasonable space groups to search for the low-lying minima in the lattice energy surface. The B3LYP/6-31G (d) level-optimized ground-state geometry is considered as the input structure for the polymorph search. The high-density polymorph is sorted from the large number of potential crystal structures, and lattice parameters for this are given in Table 2.

We can see that the energies lie in the range 66.91 to 68.52 kJ mol^{-1} cell^{-1} and the structure with $P2_1/C$ symmetry has the lowest energy. Therefore, TTTO tends to exist in the $P2_1/C$ space group (Figure 2) since the stable polymorph usually possesses lower Gibbs free energy (or total energy at 0 K). The corresponding cell parameters are $Z = 4$, $a = 8.239$ Å, $b = 8.079$ Å, $c = 16.860$ Å and $\rho = 1.922$ g cm^{-3} . The title compound may exhibit good detonation performance because density is the key factor affecting the detonation properties of high energetic density compounds.

We carefully compared the density of TTTO predicted from the Compass force field (1.922 g cm^{-3}) and from the volume inside an electron density contour of 0.001 e Bohr⁻³ using the Monte Carlo method (2.020 g cm^{-3}). Because the density of TTTO predicted inside an electron density contour of 0.001 e Bohr⁻³ using the Monte Carlo method is calculated by molecular volume of gas state, not of crystal state, the calculated molecular density of TTTO has some deviation. Therefore, we believe the crystal density predicted from the Compass force field for TTTO is more reliable.

Heat of formation

The HOF is usually taken as an indicator of the “energy content” of high energy density compounds and is one of the most important thermochemical properties of energetic materials. The DFT method has proved reliable for estimating HOF through appropriate reactions.^{46,47} In this study, the HOF of TTTO was calculated with the help of the following reaction:

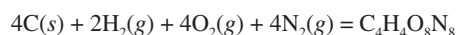
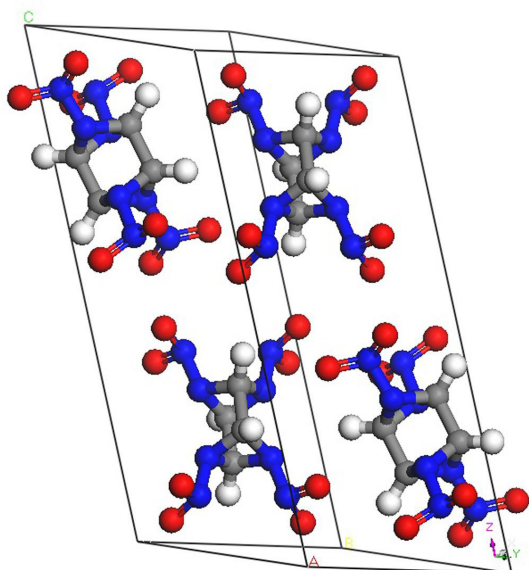


Table 2. Unit cell parameters of the possible molecular packings of TTTO

Space groups	$P2_1/C$	$P2_12_12_1$	$P-1$	$Pna2_1$	$P2_1$	$C2/C$	$Pbca$
Z	4	4	4	6	6	8	8
$E(\text{kJ mol}^{-1} \text{ cell}^{-1})$	66.91	66.98	67.66	67.49	68.19	67.96	68.52
$\rho (\text{g cm}^{-3})$	1.922	1.918	1.928	1.957	1.889	1.929	1.873
$a (\text{Å})$	8.239	8.024	6.437	12.825	12.267	10.285	8.661
$b (\text{Å})$	8.079	8.276	15.131	7.960	9.605	7.658	30.802
$c (\text{Å})$	16.860	15.233	6.804	9.711	6.477	26.098	7.768
$\alpha (^\circ)$	90.00	90.00	106.35	90.00	90.00	90.00	90.00
$\beta (^\circ)$	115.88	90.00	88.04	90.00	137.71	101.84	90.00
$\gamma (^\circ)$	90.00	90.00	126.56	90.00	90.00	90.00	90.00

**Figure 2.** Molecular packing of TTTO in $P2_1/C$ space group

With the calculated enthalpies of all species and experimental sublimation enthalpy of graphite, it is easy to obtain the HOF of TTTO. The related data are summarized in Table 3. It is found that $\Delta_f H_{\text{gas}}$ calculated by B3LYP/6-311+G(d,p) is larger than those by B3LYP/6-311G(d,p) and B3LYP/6-31G(d), with differences of 48.15 and 89.70 kJ/mol, respectively. Moreover, in comparison with the $\Delta_f H_{\text{gas}}$ from the 6-311+G(d,p) basis set at the B3LYP level, the 6-311G(d,p) basis set produces a very close value and the 6-31G(d) basis set yields a lower value by 41.55 kJ/mol. The maximum discrepancy of $\Delta_f H_{\text{gas}}$ due to using different basis sets is 48.15 kJ/mol. The $\Delta_f H_{\text{gas}}$ calculated by B3P86/6-311+G(d,p) is the largest (978.03 kJ/mol). Therefore, $\Delta_f H_{\text{gas}}$ is slightly affected by the basis sets. The result of 776.68 kJ mol⁻¹ (B3LYP/6-31G(d)) is larger than that of CL-20 (691.30 kJ mol⁻¹)⁸ and benefits heat release during detonation. This may be due to the large strain energy together with the

Table 3. Calculated total energies E_0 (a.u.) and gas-phase heats of formation $\Delta_f H_{\text{gas}}$ (kJ×mol⁻¹) for the preference compounds^a

	E_0 [C(g)]	E_0 (H ₂)	E_0 (O ₂)	E_0 (N ₂)	E_0 (C ₄ H ₄ O ₈ N ₈)	$\Delta_f H_{\text{gas}}$
B3LYP/6-31G(d)	-37.84629	-1.16534	-150.31630	-109.51853	-1193.841829	776.68
B3LYP/6-311G(d,p)	-37.88895	-1.16950	-150.29890	-109.55035	-1194.062643	818.23
B3LYP/6-311+G(d,p)	-37.89191	-1.16950	-150.30526	-109.55412	-1194.096663	866.38
B3P86/6-311+G(d,p)	-37.88345	-1.20509	-150.47791	-109.59247	-1194.935440	978.03

^a E_0 is the total energy after correction of the zero-point energy.

energy content of the C–N bonds in the rigid skeleton. Therefore, the high energy content of the title compound satisfies the necessary characteristic of energetic materials.

Infrared spectra

A scaled factor of 0.96 is adopted for these frequencies because DFT-calculated harmonic vibrational frequencies are usually larger than those observed experimentally.⁴⁸ Figure 3 depicts the simulated IR spectrum of TTTO at the B3LYP/6-31G(d). For TTTO, it is clear from Figure 3 that there are four main characteristic regions. The peak at 840 cm⁻¹ is composed of the C–H scissoring in plane. The weak peaks of less than 900 cm⁻¹ are mainly caused by the deformation of heterocycle skeleton and the bending vibration of C–H and C–C bonds. The band at 920 cm⁻¹ is composed of the N–N asymmetric stretch of heterocycle skeleton together with C–H twisting out of plane. The strongest peak in this region appears at 920 cm⁻¹ for the title compound and 960 cm⁻¹ for CL-20. At 1020 cm⁻¹ for TTTO, the weak peak is caused by the C–N stretch of the heterocycle skeleton. The remarkable signal centered at 1640 cm⁻¹ is associated with the N=O asymmetric stretch of nitro groups while the strong characteristic peak at 1330 cm⁻¹ is attributed to the C–H wagging in plane. Another remarkable signal centered at 1320 cm⁻¹ is associated with a C–N stretch and N=O symmetric stretch motion. The modes in 3000–3215 cm⁻¹ are associated with the C–H stretch. In this region, the strongest characteristic peak is found at 3100 cm⁻¹.

Thermodynamic properties

Based on the scaled vibrational results, principle of statistic thermodynamics and self-compiled program, the thermodynamic properties ranging from 200 to 800 K were obtained and listed in Table 4.

The correlation equations between the thermodynamic functions and temperature in the 200–800 K range are shown as follows and expressed in Figure 4.

The dependences of thermodynamic functions on temperature were analyzed and are helpful for further studies on other physical,

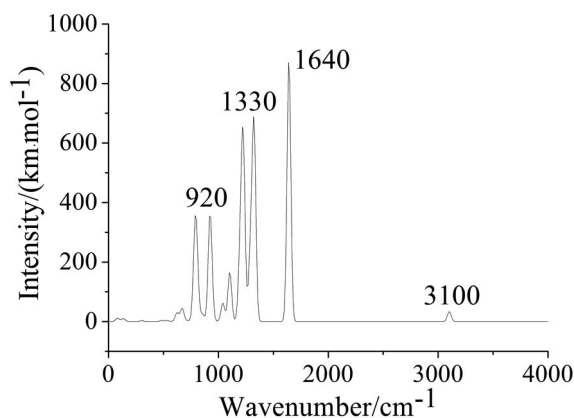


Figure 3. Calculated IR spectra of TTTO at B3LYP/6-31G (d) level

Table 4. Thermodynamic properties of TTTO at different temperatures

T/K	$C_{p,m}^\theta$ /J mol ⁻¹ K ⁻¹	S_m^θ /J mol ⁻¹ K ⁻¹	H_m^θ /kJ mol ⁻¹
200.0	186.91	460.09	23.20
298.1	257.45	547.84	45.00
300.0	258.75	549.43	45.48
400.0	323.30	633.01	74.69
500.0	374.09	710.86	109.67
600.0	412.51	782.63	149.09
700.0	441.62	848.50	191.86
800.0	464.03	909.00	237.19

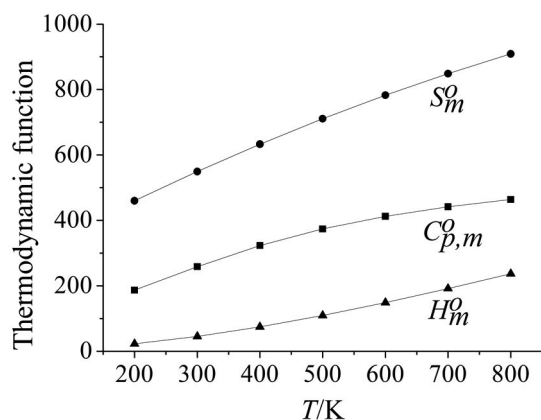


Figure 4. Relationships between thermodynamic functions ($C_{p,m}^\theta$, S_m^θ and H_m^θ) and temperature (T) for TTTO

chemical and energetic properties of TTTO. The correlation equations are as follows:

$$C_{p,m}^\theta = 9.63 + 0.99T - 5.35 \times 10^{-4}T^2$$

$$S_m^\theta = 263.83 + 1.04T - 2.92 \times 10^{-4}T^2$$

$$H_m^\theta = -13.48 + 0.13T + 2.28 \times 10^{-4}T^2$$

The corresponding correlation coefficients are 0.9997, 1.0000, and 0.9997, respectively. From these data, it is evident that all the thermodynamic functions increase with temperature.

This is because the main contributions to thermodynamic functions are from the translations and rotations of molecules when temperature is low. However, at higher temperatures, the vibrational movement is intensified and therefore makes greater contributions

to thermodynamic properties, leading to the increase in thermodynamic functions. It follows that, as the temperature increases, the gradients of $C_{p,m}^\theta$ and S_m^θ decrease, while that of H_m^θ increases constantly. The relationship between the thermodynamic functions and temperature renders the evaluation of the thermodynamic functions at different temperatures very easy and necessary for predicting reactive properties at various temperatures. For the decomposition reaction $C_4H_4O_8N_8(g) + O_2(g) \rightarrow 4CO_2(g) + 4N_2(g) + 2H_2O(g)$, both the enthalpy change and the free energy change ($\Delta G = \Delta H - T\Delta S$) can be evaluated on the basis of the thermodynamic functions. At 400 K, the enthalpy change and free energy change are 41.32 and -464.53 kJ/mol, while at 800 K values are 19.17 and -964.66 kJ/mol, respectively. This indicates that the decomposition reaction becomes less endothermic with increasing temperature. Moreover, the free energy changes appear to be much larger as the temperature increases and thus the reaction is more favorable at higher temperatures. Our previous study on the thermodynamic properties of caged compounds has proved that the calculated results have good concordance with the experimental values.⁴⁹ Because there are no experimental values for TTTO, our results may be used as a reference for experimental work and further studies on the physical and chemical properties of TTTO.

Detonation performance

The detonation velocity (D) and detonation pressure (P) of TTTO were computed by Kamlet-Jacobs empirical equations on the basis of crystal density (ρ) and calculated gas phase heat of formation at the B3LYP/6-31G(d), which are the key parameters for evaluating performances of explosion of energetic materials. Because detonation pressure and detonation velocity are calculated by HOF of gas state, not of crystal state, the calculated detonation properties of TTTO show some deviation.⁵² Although the error or limitation of the calculation method cause the predicted D and P to deviate somewhat from experiments, these results are still reliable and meaningful.

Table 5 summarizes the detonation properties of TTTO, HMX as well as CL-20. In comparison with the explosive HMX, TTTO exhibits much better detonation performance ($\rho = 1.92$ g/cm³, $D = 9.79$ km/s, $P = 44.22$ GPa) and performs similarly to CL-20. Therefore, the above prediction indicates that TTTO appears to be a promising candidate comparable to the nitramine explosive HMX and CL-20. According to energy criterion for HEDC, i.e., $\rho \approx 1.90$ g/cm³, $D \approx 9.0$ km/s, and $P \approx 40.0$ GPa, it is evident from Table 5 that TTTO satisfies requirements as a novel high energy density compound.

Table 5. Detonation properties of TTTO, HMX and CL-20

Molecule	V (cm ³ /mol)	ρ (g/cm ³)	D (km/s)	P (Gpa)
TTTO	151.93	1.92	9.79	44.22
HMX	155.79	1.90 ^a (1.92) ^b	9.10 (8.96)	39.40 (35.96)
CL-20	222.48	1.97 ^c (2.04) ^d	9.73 (9.38)	44.64

^a The calculated values are taken from ref. 23. ^b The values in parenthesis are experimental values taken from ref. 50. ^c Calculated value from ref. 8. ^d Experimental value from ref. 51.

Thermal stability

Bond dissociation energy (BDE) provides useful information for understanding the stability of energetic compounds. Generally, the lower the energy required for breaking a bond, the weaker the bond, and the easier the bond becomes a trigger bond; that is to say, the corresponding compound is more unstable, and has greater sensitivity. There is a current consensus that nitro groups often represent the

primary cause of initiation reactivity of organic polynitro compounds.⁵³⁻⁵⁵ Therefore, we selected the weakest bonds (N–N bonds) as the breaking bond based on the bond overlap populations in order to calculate BDE at the B3LYP/6-31G(d) level. The calculated BDE_{ZPE} value indicates the relative sensitivity of TTTO. The initial step should be via N–NO₂ cleavage in thermal decomposition.

Considering the practical requirements and based on the results of these studies, a quantitative criteria associated with stability (BDE of the trigger bond) requirement, i.e., BDE≈80-120 kJ/mol,⁵⁶ is proposed and employed to screen and recommend potential HEDCs. The BDE_{ZPE} value of TTTO (99.06 kJ/mol) essentially satisfies this requirement. By analyzing the structure of the title compound, it is easy to determine that TTTO has a symmetric structure. The symmetry delocalizes π electron cloud density of the system, which make BDE_{ZPE} of TTTO increase. This shows that the structure of TTTO has a great influence on thermal stability. The above investigations provide important theoretic information for molecular design of high energetic density compounds.

CONCLUSIONS

In this study, density functional theory and molecular mechanics methods were employed to study the molecular geometry, electronic structure, IR spectrum, thermodynamic functions, heat of formation, detonation performance and thermal stability of a novel high energy density compound, 3,6,7,8-tetranitro-3,6,7,8-tetraaza-tricyclo [3.1.1.1^{2,4}]octane (TTTO). The most likely packing structure belongs to the $P2_1/C$ space group. Results of detonation velocity and detonation pressure calculations indicated that TTTO ($\rho = 1.92$ g/cm³, $D = 9.79$ km/s, $P = 44.22$ GPa) performs similarly to CL-20, which essentially satisfies the quantitative criteria for the energy as a HEDC. An analysis of bond dissociation energies for several relatively weak bonds suggests that N–NO₂ bond is the weakest and may occur in thermal decomposition. These results provide theoretical support for molecular design and experimental synthesis of HEDCs.

ACKNOWLEDGMENTS

This work was supported by the NSAF Foundation of National Natural Science Foundation of China and the China Academy of Engineering Physics (Grant No.: 11076017).

REFERENCES

- Santamaria, R.; Mondragon-Sanchez, J. A.; Bokhimi, X.; *J. Phys. Chem. A* **2012**, *116*, 3673.
- Zhang, J. Y.; Du, H. C.; Wang, F.; Gong, X. D.; Huang, Y. S.; *J. Phys. Chem. A* **2011**, *115*, 6617.
- Hou, J. G.; Cao, R.; Wang, Z.; Jiao, S. Q.; Zhu, H. M.; *J. Hazard. Mater.* **2012**, *217*, 177.
- Wang, F.; Du, H. C.; Zhang, J. Y.; Gong, X. D.; *J. Phys. Chem. A* **2011**, *115*, 11788.
- Bushuyev, O. S.; Brown, P.; Maiti, A.; Gee, R. H.; Peterson, G. R.; Weeks, B. L.; Hope-Weeks, L. J.; *J. Am. Chem. Soc.* **2012**, *134*, 1422.
- Rahm, M.; Dvinskikh, S. V.; Furo, I.; Brinck, T.; *Angew. Chem., Int. Ed.* **2011**, *50*, 1145.
- Talawar, M. B.; Sivabalan, R.; Mukundan, T.; Muthurajan, H.; Sikder, A. K.; Gandhe, B. R.; Rao, A. S.; *J. Hazard. Mater.* **2009**, *161*, 589.
- Ghule, V. D.; Jadhav, P. M.; Patil, R. S.; Radhakrishnan, S.; Soman, T.; *J. Phys. Chem. A* **2010**, *114*, 498.
- Bayat, Y.; Mokhtari, J.; *Defence Sci. J.* **2011**, *61*, 171.
- Odbadrakh, K.; Lewis, J. P.; Nicholson, D. M.; *J. Phys. Chem. C* **2010**, *114*, 7535.
- Zhang, M. X.; Eaton, P. E.; Gilardi, R.; *Angew. Chem., Int. Ed.* **2000**, *39*, 401.
- Ravi, P.; Gore, G. M.; Sikder, A. K.; Tewari, S. P.; *Int. J. Quantum. Chem.* **2012**, *112*, 1667.
- Sharia, O.; Kuklja, M. M.; *J. Phys. Chem. B* **2012**, *115*, 12677.
- Sollot, G. P.; Gilbert, E. E.; *J. Org. Chem.* **1980**, *45*, 5405.
- Maksimowski, P.; Fabijanska, A.; Adamiak, J.; *Propellants Explos. Pyrotech.* **2010**, *35*, 353.
- Bayat, Y.; Hajimirsadeghi, S. S.; Pourmortazavi, S. M.; *Org. Process. Res. Dev.* **2011**, *15*, 810.
- Lin, C. P.; Chang, C. P.; Chou, Y. C.; Chu, Y. C.; Shu, C. M.; *J. Hazard. Mater.* **2010**, *176*, 549.
- Qiu, L.; Xiao, H. M.; Gong, X. D.; Ju, X. H.; Zhu, W. H.; *J. Phys. Chem. B* **2006**, *110*, 3797.
- Xu, X. J.; Xiao, H. M.; Ju, X. H.; Gong, X. D.; Zhu, W. H.; *J. Phys. Chem. A* **2006**, *110*, 5929.
- Richard, R. M.; Ball, D. W.; *J. Mol. Struct.* **2008**, *858*, 85.
- Zhang, X. W.; Zhu, W. H.; Xiao, H. M.; *J. Phys. Chem. A* **2010**, *114*, 603.
- Wei, T.; Zhu, W. H.; Zhang, X. W.; Li, Y. F.; Xiao, H. M.; *J. Phys. Chem. A* **2009**, *113*, 9404.
- Turker, L.; Atalar, T.; Gumus, S.; Camur, Y.; *J. Hazard. Mater.* **2009**, *167*, 440.
- Zhang, G. H.; Zhao, Y. F.; Hao, F. Y.; Zhang, P. X.; Song, X. D.; *Int. J. Quantum. Chem.* **2009**, *109*, 226.
- Becke, A. D.; *J. Chem. Phys.* **1992**, *97*, 9173.
- Lee, C.; Yang, W.; Parr, R. G.; *Phys. Rev. B* **1988**, *37*, 785.
- Becke, A. D.; *J. Chem. Phys.* **1993**, *98*, 5648.
- Frisch, M. J.; Trucks, G. W.; Schlegel, H. B.; Scuseria, G. E.; Robb, M. A.; Cheeseman, J. R.; Zakrzewski, V. G.; Montgomery, J. A.; Stratmann, R. E.; Burant, J. C.; Dapprich, S.; Millam, J. M.; Daniels, A. D.; Kudin, K. N.; Strain, M. C.; Farkas, O.; Tomasi, J.; Barone, V.; Cossi, M.; Cammi, R.; Mennucci, B.; Pomelli, C.; Adamo, C.; Clifford, S.; Ochterski, J.; Petersson, G. A.; Ayala, P. Y.; Cui, Q. K.; Morokuma, D. K.; Malick, A. D.; Rabuck, K.; Raghavachari, J. B.; Foresman, J. C.; Ortiz, J. V.; Baboul, A. G.; Stefanov, B. B.; Liu, G.; Liashenko, A.; Piskorz, P.; Komaromi, I.; Gomperts, R.; Martin, R. L.; Fox, D. J.; Keith, T.; Al-Laham, M. A.; Peng, C. Y.; Nanayakkara, A.; Gonzalez, C.; Challacombe, M.; Gill, P. M. W.; Johnson, B.; Chen, W.; Wong, M. W.; Andres, J. L.; Gonzalez, C.; Head-Gordon, M.; Replogle, E. S.; Pople, J. A.; *Gaussian 03*, 2003, Gaussian, Inc.: Pittsburgh, PA.
- Hill, T. L.; *Introduction to Statistic Thermodynamics*, Addison-Wesley: New York, 1960.
- Kamlet, M. J.; Jacobs, S. T.; *J. Chem. Phys.* **1968**, *48*, 23.
- Zhang, X. H.; Yun, Z. H.; *Explosive Chemistry*, National Defence Industry Press: Beijing, 1989.
- Politzer, P.; Murray, J. S.; *J. Mol. Struct.* **1996**, *376*, 419.
- Lide, D. R.; *CRC Handbook of Chemistry and Physics*, CRC Press LLC: Boca Raton, 2002.
- Materials Studio 4.4; *Accelrys*, 2008.
- Chernikova, N. Y.; Belsky, V. K.; Zorkii, P. M.; *J. Struct. Chem.* **1990**, *31*, 661.
- Mighell, A. D.; Himes, V. L.; Rodgers, J. R.; *Acta Crystallogr., Sect. A: Found. Crystallogr.* **1983**, *39*, 737.
- Srinivasan, R.; *Acta Crystallogr., Sect. A: Found. Crystallogr.* **1992**, *48*, 917.
- Baur, W. H.; Kassner, D.; *Acta Crystallogr., Sect. B: Struct. Sci.* **1992**, *48*, 356.
- Cao, X. Z.; Song, T. Y.; Wang, X. Q.; *Inorganic Chemistry*, Higher Education Press: Beijing, 1987.
- Archibald, T. G.; Gilardi, R.; Baum, K.; George, C.; *J. Org. Chem.* **1990**, *55*, 2920.

41. Wang, G. X.; Shi, C. H.; Gong, X. D.; Zhu, W. H.; Xiao, H. M.; *J. Hazard. Mater.* **2009**, *169*, 813.
42. Xu, X. J.; Zhu, W. H.; Xiao, H. M.; *J. Mol. Struct. (Theochem)* **2008**, *853*, 1.
43. Sun, H.; *J. Phys. Chem. B* **1998**, *102*, 7338.
44. Xu, X. J.; Zhu, W. H.; Xiao, H. M.; *J. Phys. Chem. B* **2007**, *111*, 2090.
45. Xu, X. J.; Zhu, W. H.; Xiao, H. M.; *Chin. J. Chem.* **2008**, *26*, 602.
46. Jursic, B. S.; *J. Chem. Phys.* **1997**, *106*, 2555.
47. Jursic, B. S.; *J. Mol. Struct.* **1997**, *391*, 75.
48. Scott, A. P.; Radom, L.; *J. Phys. Chem.* **1996**, *100*, 16502.
49. Qiu, L. M.; Ye, D. Y.; Wei, W.; Chen, K. H.; Hou, J. X.; Zheng, J.; Gong, X. D.; Xiao, H. M.; *J. Mol. Struct. (Theochem)* **2008**, *866*, 63.
50. Agrawal, J. P.; Hodgson, R. D.; *Organic Chemistry of Explosives*, John Wiley & Sons, 2007.
51. Sikder, A. K.; Sikder, N.; *J. Hazard. Mater.* **2004**, *112*, 1.
52. Politzer, P.; Murray, J. S.; *Cent. Eur. J. Energet. Mater.* **2011**, *3*, 209.
53. Owens, F. J.; Jayasuriya, K.; Abrahmsen, L.; Politzer, P.; *Chem. Phys. Lett.* **1985**, *116*, 434.
54. Michels, H. H.; Montgomery, J. A.; *J. Phys. Chem.* **1993**, *97*, 6602.
55. Murray, J. S.; Concha, M. C.; Politzer, P.; *Mol. Phys.* **2009**, *107*, 89.
56. Chung, G.; Schmidt, M. W.; Gordon, M. S.; *J. Phys. Chem. A* **2000**, *104*, 5647.